Desalination and Water Treatment
www.deswater.com
15 (2010) 11–19
March
1944-3994 / 1944-3986 © 2010 Desalination Publications. All rights reserved.
doi: 10.5004/dwt.2010.1661

A rapid performance diagnosis of seawater reverse osmosis membranes: simulation approach

Young Geun Lee[a], Do Yeon Kim[b], Yu Chang Kim[c], Yun Seok Lee[a], Da Hee Jung[a], Minkyu Park[a], Sang-Jin Park[c], Sangho Lee[d], Dae Ryook Yang[b], Joon Ha Kim[a,e,f]*

[a]*Department of Environmental Science and Engineering, Gwangju Institute of Science and Technology (GIST), Gwangju, 500-712, Korea*
Tel. +82 62 970-3277; Fax +82 62 970-2434; email: joonkim@gist.ac.kr
[b]*Department of Chemical & Biological Engineering, Korea University, Seoul, 136-701, Korea*
[c]*Energy Plant Research Division, Korea Institute of Machinery & Materials, Daejeon, Korea*
[d]*Korea Institute of Construction Technology, 2311 Daehwa-Dong, Ilsan-gu, Kyonggi-do, Korea*
[e]*Center for Seawater Desalination Plant, GIST, Gwangju, 500-712, Korea*
[f]*Sustainable Water Resource Technology Center, GIST, Gwangju, 500-712, Korea*

Received 12 November 2009; Accepted in revised form 24 December 2009

ABSTRACT

Recovery and salt rejection rate, which are directly related to the membrane properties and operating conditions (i.e., feed flow rate, pressure, temperature, and TDS concentration), are two main indicators for evaluating the performance of a reverse osmosis (RO) membrane process. A simple and rapid test with minimum data is inevitably requested to diagnose membrane performance at a certain operating conditions, because experiments at all operating conditions are inefficient and consumable work in the view of cost as well as man-hour. In this study, permeate flow rate and TDS concentration of three kinds of commercial RO membranes were carefully examined under various operating conditions [i.e., feed pressure (45–65 kgf/cm^2) and temperature (5–30°C)]. Based on the experimental data, membrane resistance models including temperature and pressure correction factors were developed for the rapid diagnosis of SWRO membrane performances. As a result, the models developed in this study have good agreements between observed and simulated data. Based on the procedure in this study, the performance of any type of RO membranes can be rapidly examined by simple model parameter inputs. Furthermore, the developed diagnosis tool for performance test of SWRO membranes can be practically applied to build database of membrane performance for designing the SWRO process with minimum data as well as to reduce the cost and effort for data acquisition.

Keywords: Reverse osmosis membrane; Membrane resistance model; Temperature correction factor; Pressure correction factor

* Corresponding author.

Presented at SeaHERO Academic Workshop on Development and Optimization of SWRO Desalination Systems Korea University, Seoul, Korea, November 13–14, 2009

1. Introduction

Reverse osmosis (RO) is a pressure-driven separation process, which is capable of passing water while rejecting solutes (i.e., salts or low molecular weight organics) [1]. Recently, seawater reverse osmosis (SWRO) desalination processes have been widely adapted in the worldwide, because it is more economically feasible than distillation desalination processes such as multi-stage flash (MSF) and multi-effect distillation (MED) [2]. Furthermore, since a number of researches related to energy saving and cost reduction in SWRO desalination process have been carried out, it is expected that the production cost of fresh water can be continually reduced, leading to more expansion of the SWRO desalination process for fresh water production from seawater [3–8].

As demands for constructing SWRO plants have been increasing, the necessity of RO models (e.g., deterministic and stochastic models) has also increased to simulate accurate membrane performances for the purpose of efficient plant design and operation management. Until now, A number of models have been proposed for simulating and predicting performances of SWRO desalination process such as irreversible thermodynamic models, solution-diffusion model, porous model, membrane resistance model, and so on [9,10]. Among RO models, membrane resistance model was used in this study. The membrane resistance (R_m) representing membrane characteristic has a role of restriction of passing the permeate flux. In other research, this model was extensively applied to discribe membrane fouling as resistance-in-series model [11]. As an empirical model, the membrane resistance which has different value according to kinds of membrane in the model can be estimated based on the experiments. Therefore, the model can analyze and simulate a particular performance of membrane using estimated parameters.

Membrane performance tests are inevitable for investigating whether a membrane has acceptable/considerable performances at several operating conditions (i.e., variations of feed pressure, flow rate, temperature, and concentration) including extreme cases (e.g., extremely low temperature). However, to test the membrane performance at all the operating conditions is obviously inefficient and consumable work in the view of cost and manpower for experiments. Therefore, a RO performance simulator developed with minimum operating conditions can be a considerably useful tool to investigate most of the operating cases within the range of minimum and maximum operating conditions. Comparing to other studies using membrane resistance model [11,12], in this study, modified membrane resistance model was applied to simulate performances of commertial SWRO membranes. For enhancing the accuracy of the model, the permeate velocity described by Darcy's law was modified using temperature correction factor (TCF) as a type of Arrhenius' form for reflecting the effect of temperature and pressure [13]. In addition, TCF and pressure correction factor (PCF) are added to rejection rate.

The objectives of this study are: 1) to develop the modified resistance model including correction factors (i.e., TCF and PCF); 2) to investigate the performances of three commercial membranes using developed models; and 3) to suggest a simulation approach for performance diagnosis of various SWRO membranes based on the minimum parameter inputs.

2. Data acquisition

2.1. Pilot system

Fig. 1 shows the configuration and photograph of pilot system in this study. In the RO pilot system, feed water is first pretreated to avoid membrane fouling using both sand and cartridge filters. And then it is sent to two stage 4″ RO units by a high pressure pump. Finally, the permeated and concentrated waters go into the feed tank instead of storage tank for a recycle purpose. The three kinds of commercial spiral-wound reverse osmosis membranes (i.e., Membrane A, Membrane B, and Membrane C) were used in the experiments, which have the membrane area of 6.9, 6.5, and 6.9 m^2, respectively. Both

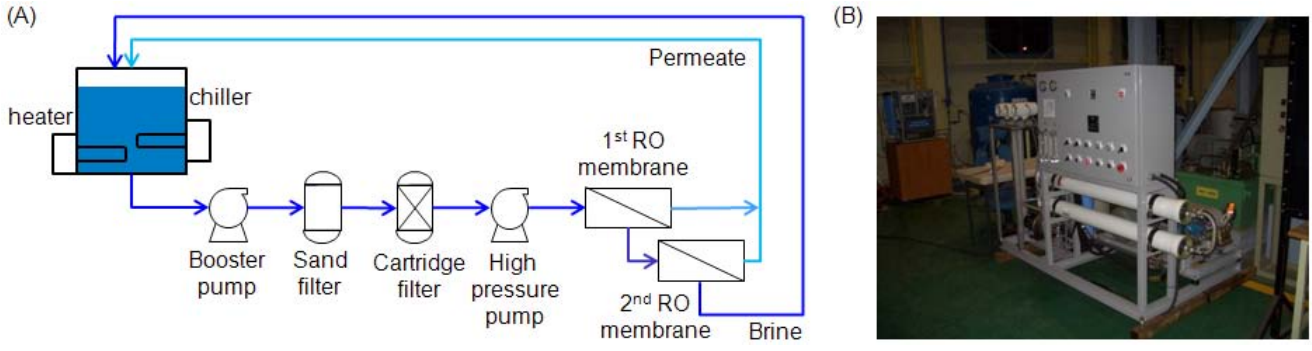

Fig. 1. Schematic diagram (A) and photograph (B) of SWRO lab-scale pilot system.

heater and chiller connected to feed tank were used for modulating the feed temperature. And high pressure pump and a brine valve were utilized for controlling the feed flow rate and pressure.

2.2. Experimental data

Tables 1 and 2 show experimental data set for investigating the effect of feed pressure and water temperature on the membrane performance. 10 operating conditions [feed pressure variations (45–65 kgf/cm^2) at 20°C and feed water temperature variations (5–30°C) at 55 kgf/cm^2] were conducted at almost fixed feed flow rate of 30 LPM (liter per minute) with salt concentration of 32,000 ppm using three kinds of RO membranes. Each experiment was performed at a stable and steady operating condition. For the validation of a model, twenty operating conditions [combination of operating pressure (45–65 kgf/cm^2) and feed water temperature (5–30°C) except for upper 10 operating conditions (see bold character in Table 1)] were supplemented using Membrane A (see normal characters in Table 1). The permeate flow rate and salt concentration were measured using flow and conductivity meters, respectively. And the performances (i.e., recovery and salt rejection rates) of each membrane are summarized in Tables 1 and 2.

Table 1
Experimental data of Membrane A

				Permeate		Output parameter	
Temperature (°C)	Pressure (kgf/cm^2)	Flow rate (LPM)	TDS (ppm)	Flow rate (LPM)	TDS (ppm)	Recovery rate (%)	Rejection rate (%)
5	45	30.2	31400	3.7	97.1	12.33	99.70
5	50	30.2	31300	4.7	79.5	15.67	99.75
5	**55**	**30.1**	**31300**	**5.6**	**73.1**	**18.73**	**99.77**
5	60	30.0	31500	6.3	64.1	21.14	99.80
5	65	29.9	31400	7.1	59.1	23.83	99.82
10	45	30.2	31700	2.8	82.4	9.27	99.74
10	50	30.0	31600	3.4	66.4	11.33	99.79
10	**55**	**30.0**	**31600**	**4.0**	**57.8**	**13.33**	**99.82**
10	60	29.9	31600	4.6	53.1	15.38	99.83
10	65	29.8	31400	5.2	45.0	17.45	99.86
15	45	30.1	31900	3.3	85.6	10.96	99.73
15	50	30.0	31700	4.0	70.1	13.3	99.78
15	**55**	**29.9**	**31700**	**4.7**	**61.6**	**15.72**	**99.81**
15	60	29.9	31900	5.4	54.6	18.06	9.83
15	65	29.8	31900	6.1	50.7	20.47	99.84
20	**45**	**30.0**	**32100**	**3.7**	**97.1**	**12.33**	**99.70**
20	**50**	**30.0**	**32100**	**4.7**	**79.5**	**15.67**	**99.75**
20	**55**	**29.9**	**32000**	**5.5**	**71.7**	**18.39**	**99.78**
20	**60**	**29.8**	**32000**	**6.3**	**64.1**	**21.14**	**99.80**
20	**65**	**29.8**	**32000**	**7.1**	**59.1**	**23.83**	**99.82**
25	45	29.9	32000	4.2	104.6	14.05	99.67
25	50	29.9	32000	5.2	87.1	17.39	99.73
25	**55**	**29.8**	**32100**	**6.3**	**79.5**	**21.14**	**99.75**
25	60	29.8	32000	7.1	70.9	23.83	99.78
25	65	29.6	32000	8.0	64.8	27.03	99.80
30	45	29.9	32100	4.7	121.6	15.72	99.62
30	50	29.8	32100	5.9	101.2	19.80	99.68
30	**55**	**29.8**	**32100**	**6.9**	**91.1**	**23.15**	**99.72**
30	60	29.7	32000	7.9	84.0	26.60	99.74
30	65	29.6	32000	8.8	77.3	29.73	99.76

Bold character, basic operation conditions for developing a model.
Normal character, supplemented operation conditions for validating a developed model.

Table 2
Experimental data of Membrane B and Membrane C

Membrane	Feed				Permeate		Output parameter	
	Temperature (°C)	Pressure (kgf/cm^2)	Flow rate (LPM)	TDS (ppm)	Flow rate (LPM)	TDS (ppm)	Recovery rate (%)	Rejection rate (%)
Membrane B	20	45	30.1	32100	4.3	176.6	14.29	99.45
	20	50	30.0	32200	5.4	153.3	18.00	99.52
	20	55	30.0	32100	6.3	138.7	21.00	99.57
	20	60	29.9	32000	7.3	129.4	24.42	99.60
	20	65	29.8	31600	8.2	126.4	27.52	99.60
	5	55	30.1	31700	4.1	103.1	13.62	99.68
	10	55	30.0	31700	4.7	112.4	15.67	99.65
	15	55	30.0	31900	5.4	123.6	18.00	99.61
	25	55	29.9	32100	7.0	173.2	23.4	99.46
	30	55	29.8	32100	7.7	204.0	25.8	99.36
Membrane C	20	45	30.1	32200	3.6	135.3	11.96	99.58
	20	50	30.0	32100	4.5	113.2	15.00	99.65
	20	55	30.0	32000	5.4	102.9	18.00	99.68
	20	60	29.9	32200	6.1	94.9	20.40	99.71
	20	65	29.8	31900	6.8	92.0	22.82	99.71
	5	55	30.2	31400	3.2	59.0	10.60	99.81
	10	55	30.1	31600	3.9	68.5	12.96	99.78
	15	55	30.0	31900	4.6	84.1	15.33	99.74
	25	55	29.9	32000	6.1	131.0	20.40	99.59
	30	55	29.9	32100	6.7	162.1	22.41	99.50

3. Model development

In this study, the SWRO model is developed to simulate the membrane performance. Fig. 2 shows a simplified schematic diagram of a channel with a membrane at one side and the variables used in the study: *L*, *W*, and *H* denote the length, width, and height of the channel, respectively; $u(x)$ and $v(x)$ are cross and permeate flow velocity at local position (x) being the distance from the inlet. The channel length (L) can be lengthened according to the number of RO membrane elements (n) in a vessel for customary practice with several modules in series. Basic transport equations and mathematical models for spiral wound module are discussed in detail below.

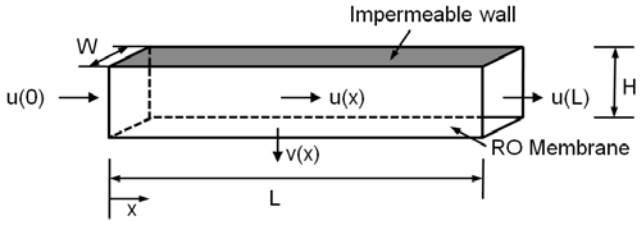

Fig. 2. Schematic diagram of spiral wound reverse osmosis membrane: *L*, *W*, and *H* indicate channel length, width, and height, respectively; *u* and *v* indicate crossflow and permeate flow velocity, respectively; *x* shows the longitudinal direction.

From the principle of membrane transfer, the local permeate flux in the membrane resistance model is shown as:

$$v(x) = \frac{\Delta p(x) - \Delta\pi(x)}{R_m} \tag{1}$$

where $v(x)$, $\Delta p(x)$ and $\Delta\pi(x)$ are the permeate velocity, the transmembrane pressure (TMP), and the transmembrane osmotic pressure, respectively, at point x. R_m is the membrane resistance, which is defined as:

$$R_m = R_{m,ref} \cdot \mathrm{TCF}_{R_m} \tag{2}$$

where $R_{m.\,ref}$ is reference membrane resistance, and TCF_{Rm} is temperature correction factor for membrane resistance, which is determined as:

$$\mathrm{TCF}_{R_m} = \exp\left(a_T\left(\frac{1}{T_a} - \frac{1}{T_{ref}}\right)\right) \tag{3}$$

where a_T is temperature coefficient for TCF_{Rm}, T_a the absolute temperature, and T_{ref} the reference temperature. And TMP declines along the channel due to the friction

of the crossflow with the membrane walls and spacers in the channel, which is calculated as [12,14]:

$$\Delta p(x) = \Delta p(0) - \frac{12k\mu}{H^2}\int_0^x u(\xi)d\xi \quad (4)$$

where $\Delta p(0)$ is the TMP at inlet, H the channel height, and k the friction coefficient for spacers. μ is the dynamic viscosity of water, which is computed as a function of temperature [15].

$$\mu = 2.414\times10^{-5}\times10^{\frac{247.8}{T_a-140}} \quad (5)$$

Based on the mass conservation in the membrane channel, the crossflow velocity, $u(x)$, at any point along the channel can be determined as:

$$u(x) = u(0) - \frac{1}{H}\int_0^x v(\xi)d\xi \quad (6)$$

where $u(0)$ is an feed flow velocity, and ξ the dummy integration variable. The osmotic pressure can be calculated by the empirical equation [16].

$$\pi = \left(23745 + 64.784\times c + 1.7753\times10^{-4}c^2\right)\frac{T_a}{298} \quad (7)$$

where c the TDS concentration. By applying mass conservation in the membrane channel, TDS concentration, $c(x)$, at any point along the channel can be determined as:

$$c(x) = \frac{1}{u(x)}\left[c(0)u(0) - \frac{1-r_{rej}(x)}{H}\int_o^x c(\xi)v(\xi)d\xi\right] \quad (8)$$

where $c(0)$ is an feed TDS concentration, and r_{rej} the rejection rate. Since rejection rate of a RO membrane is changed with feed temperature and TMP, it can be a function of temperature and TMP as an Arrhenius' form to reflect the various feed condition of the SWRO plant.

$$r_{rej} = r_{rej,ref}\cdot \mathrm{TCF}_{rej}\cdot \mathrm{PCF}_{rej} \quad (9)$$

where r_{rej0} is intrinsic rejection rate, and TCF_{rej} and PCF_{rej} are temperature correction factor and pressure correction factor for the rejection rate estimation, respectively, which are determined by

$$\mathrm{TCF}_{rej} = \exp\left(b_T\left(\frac{1}{T_a} - \frac{1}{T_{ref}}\right)\right) \quad (10)$$

$$\mathrm{PCF}_{rej} = \exp\left(b_p\left(\frac{1}{\Delta p} - \frac{1}{p_{ref}}\right)\right) \quad (11)$$

where b_T is temperature coefficient for TCF_{Rm}, b_p is pressure coefficient for PCF_{Rm}, and p_{ref} is the reference pressure.

4. Results and discussion

4.1. Procedure of parameter estimation

Using the membrane resistance model regardless of TCF_{Rm} in Eq. (3), membrane resistance values are extracted at various operation conditions using Membrane A. Fig. 3A shows that R_m values are exponentially decreasing in accordance with feed temperature at constant pressure (55 kgf/cm²). However, the effect of pressure at fixed temperature condition (20°C) on variation of the membrane resistance was ignored in this study, because it is shown that it was relatively slight comparing to temperature effect. It indicates that since constant R_m representing the characteristics of membrane does not fit well to performance data including temperature variation, it is needed to insert TCF_{Rm} to the Eq. (2) as a type of Arrhenius' form. In addition, rejection rate can be a function of temperature

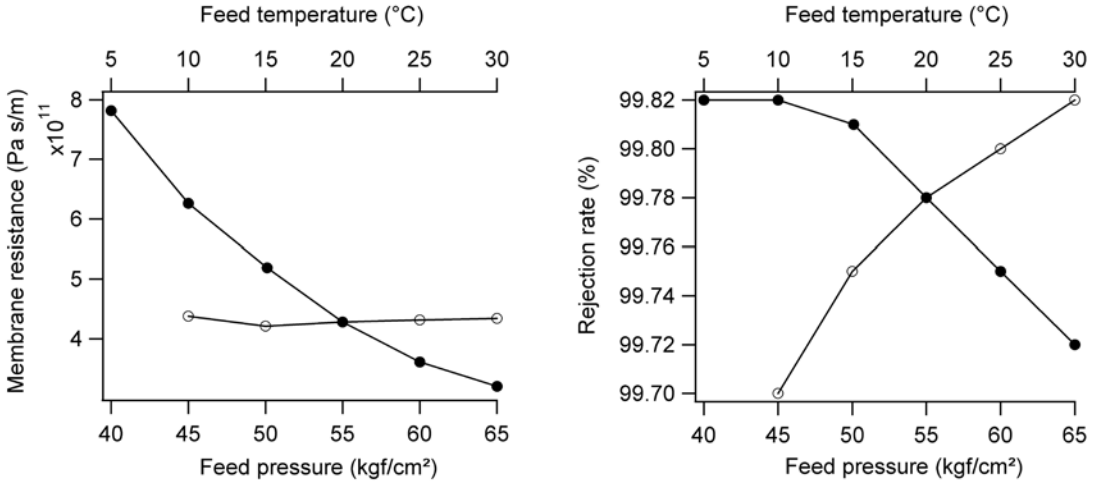

Fig. 3. The variations of membrane resistance (A) and rejection rate (B) according to the variation of temperature and pressure.

and pressure, because rejection rate varies according to the variation of temperature and pressure as shown in Fig. 3B. Therefore, rejection rate also needs correction factors such as TCF_{rej} and PCF_{rej}, which is shown in Eq. (9).

For estimating parameters in the model, the following procedure is sequentially progressed. First of all, a reference membrane resistance ($R_{m,\,ref}$) is determined at temperature 20°C and pressure 55 kgf/cm² with other operating conditions such as feed flow rate of 30 LPM and salt concentration of 32000 ppm. Then, a temperature coefficient (a_T) of TCF_{Rm} for membrane resistance can be obtained based on the experimental data ($N = 10$) including actual rejection rate at each condition shown in Tables 1 and 2. Finally, temperature (b_T) and pressure (b_p) coefficients for rejection rate are estimated using $R_{m,ref}$, a_T, $r_{rej,ref}$ (rejection rate at temperature 25°C and pressure 55 kgf/cm²) and experimental data.

4.2. Model validation

As the results, reference membrane resistances ($R_{m,\,ref}$) for Membrane A, Membrane B, and Membrane C were obtained as 4.28×10^{11}, 3.45×10^{11}, and 4.37×10^{11} Pa s/m, respectively, shown in Table 3. Temperature coefficient (a_T) for membrane resistance, and temperature (b_T) and pressure (b_p) coefficients for salt rejection rate of each membrane are also shown in Table 3. In terms of these estimated parameters, we obtained good agreement between measured and simulated values each membrane. In Table 3, R^2 values of Membrane A, Membrane B, and Membrane C were 0.99, 0.99, and 0.98 for recovery rate, and 0.95, 0.91, and 0.95 for rejection rate, respectively. Furthermore, the data which have not been used in Table 1 (normal characters) was applied to the validation of the developed model. As a result, it is shown that R^2 values of recovery (Fig. 4A) and rejection rates (Fig. 4B) between measured and simulated values are 0.99 and 0.95, respectively. It means that the developed model based on the 10 experimental conditions is enough to simulate the interpolating conditions (20 experimental conditions). That is, the number of experimental conditions for investigating the performance of membrane and suggesting appropriate operation condition for proposed water production can be reduced using the simple approach used in this study.

4.3. Model simulations

Fig. 5 shows that the performances (i.e., recovery rate and rejection rate) of membranes are simulated extensively using the models developed based on the experimental data (black circles in Fig. 5). In the view of

Table 3
Estimated parameters for three test membranes

Parameter	Membrane A	Membrane B	Membrane C
R_m: membrane resistance, Pa s/m	4.28×10^{11}	3.45×10^{11}	4.37×10^{11}
a_T: temperature coefficient for temperature correction factor, K	2518	2294	2483
$r_{rej,ref}$: reference rejection rate, %	99.78	99.57	99.68
b_T: temperature coefficient for salt rejection, K	3.20	8.65	9.30
b_p: pressure coefficient for salt rejection, Pa	–16865.71	–23436.34	–19527.20
R^2 of recovery rate	0.99	0.99	0.98
R^2 of rejection rate	0.95	0.91	0.95

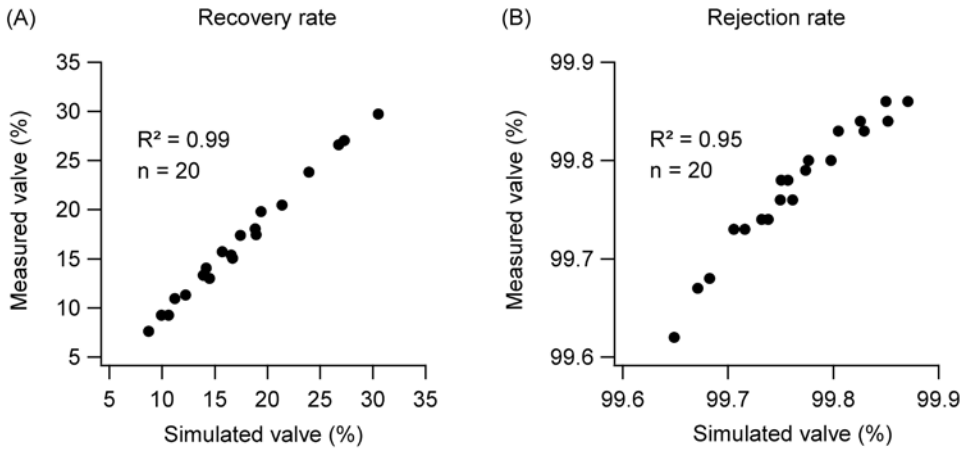

Fig. 4. Measured and simulated data of both recovery rate (A) and rejection rate (B) of Membrane A.

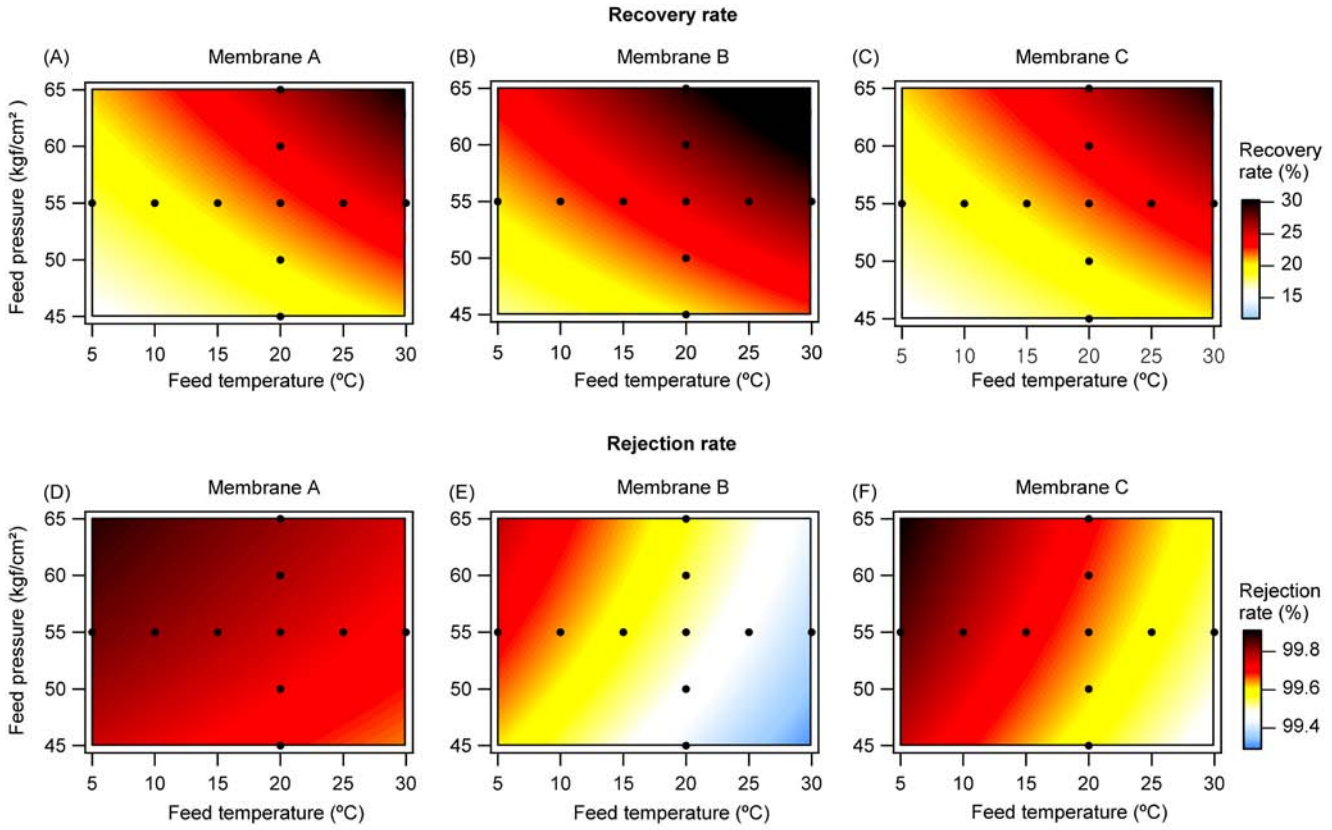

Fig. 5. Simulation results for the comparison of three test membrane performance: recovery rate of (A) Membrane A, (B) Membrane B, and (C) Membrane C; rejection rate of (D) Membrane A, (E) Membrane B, and (F) Membrane C. 10 black circles indicate experimental data.

recovery rate (Fig.5A, B, and C), as both feed temperature and pressure increase, recovery rates of three membranes also increase. Especially, the recovery rate of Membrane B is relatively higher than those of other membranes (i.e., Membrane A and C) which have similar trend of recovery rate. When temperature is 25°C and pressure 60 kgf/cm^2, while the recovery rate of Membrane B is around 26%, those of other membranes are almost 22%.

As shown in Figs. 5D, E, and F, all membranes have higher rejection rate in accordance with the decrease of feed temperature and increase of feed pressure. As opposed to the recovery rate, Membrane B (Fig. 5D) has relatively lower rejection rate comparing to the other membranes (Figs. 5E and F). Also, even though Membrane A and Membrane C have similar recovery rate in the entire operating conditions, rejection rate of Membrane A has relatively higher than Membrane C. As shown in Fig. 5A, the difference between maximum and minimum rejection rate of Membrane A is lower than Membrane C, indicating that Membrane A can maintain relatively high rejection rate regardless of the increase of feed temperature and the decrease of feed pressure comparing to Membrane C.

From the above results, it is known that the membranes have different characteristics for freshwater production. Considering these characteristics of membrane, Membrane B can have better performance comparing to other membranes for only water quantity. However, in the view of both water quality and quantity, Membrane A is the relatively effective to produce freshwater on the same operating conditions. Therefore, it should be considered to select appropriate membranes according to a beneficial purpose of the construction criteria for the target SWRO plant.

4.4. Simulator for performance of membranes

Fig. 6 shows the schematic diagram of simple test tool for membrane performance. This simulator consists of five sections such as membrane properties, operation conditions, parameter estimations, validation, and simulation. At first, reference membrane resistance ($R_{m,ref}$) can be determined based on the membrane properties and operation conditions which are inputs for the simulator. And other parameters (i.e., temperature and pressure coefficients for TCF and PCF, respectively) can be estimated based on experimental data including 10 conditions (see bold characters in Table 1). These processes follow above

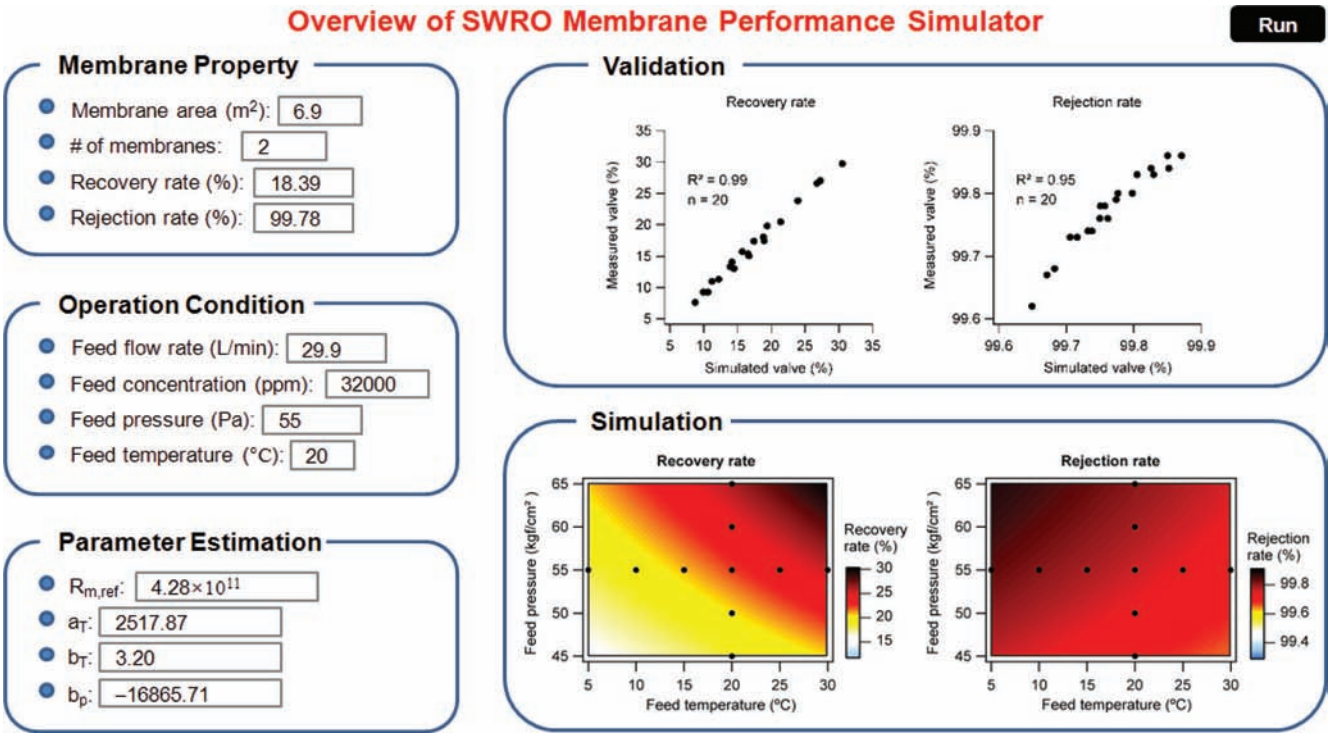

Fig. 6. Schematic diagram of overview of SWRO membrane performance simulator: membrane property, operation condition, parameter estimation, validation and simulation.

procedure of parameter estimation. The estimated values are shown in parameter estimation section. Then, this model will be validated using another data set (see normal characters in Table 1) which is different from data set for parameter estimation. Based on validation results shown in validation section, the model can be checked whether it has good agreement between measured and simulated value. Finally, in simulation section, the extended performances which are rejection and recovery rate according to temperature and pressure. The simulator developed in this study can be applied to build the database of membrane performance for plant design software.

5. Conclusions

The model used in this study can be used in any type of RO membranes with a few adjustments for model parameters (i.e., reference membrane resistance, temperature coefficient for TCF, pressure coefficient for PCF). Based on the procedure performed in this study, model parameters representing the characteristics of each membrane can be estimated for simulating performances of various membranes. The models developed with the minimum parameter inputs can be utilized to investigate the performance of membrane at other conditions and suggest the appropriate operation condition for proposed water production. The simulation approach in this study can be practically applied to build database of membrane performance for designing the SWRO plant based on the minimum data which is instead of whole data for reducing the cost and exertion of data acquisition. Furthermore, the simulator developed in this study can be easily used to test membrane performance.

Acknowledgements

This research was supported by a grant (07seaheroB02-01) from the Plant Technology Advancement Program funded by the Ministry of Land, Transport and Maritime Affairs of the Korean government.

Symbols

a_T — Temperature coefficients of TCF_{Rm}
b_T — Temperature coefficients of TCF_{rej}
b_p — Pressure coefficients of PCF_{rej}
c — TDS concentration, mg/l
H — Channel height, m
k — Friction coefficient
L — Channel length, m
p — Pressure, Pa
p_{ref} — Reference pressure, Pa
PCF_{rej} — Pressure correction factor for rejection rate
r_{rej} — Rejection rate

$r_{rej,ref}$ — Reference rejection rate
R_m — Membrane resistance, Pa s/m
$R_{m,ref}$ — Reference membrane resistance, Pa s/m
T_a — Absolute temperature, K
T_{ref} — Reference temperature, K
TCF_{R_m} — Temperature correction factor for membrane resistance
TCF_{rej} — Temperature correction factor for rejection rate
u — Crossflow velocity, m/s
v — Permeate velocity, m/s
W — Channel width, m
x — Local position, m

Greek

ξ — Dummy integration variable
π — Osmotic pressure, Pa
μ — Dynamic viscosity of water, Pa s

References

[1] S.P. Beier, Pressure Driven Membrane Processes, 2007.
[2] C. Fritzmann, J. Lowenberg, T. Wintgens and T. Melin, State-of-the-art of reverse osmosis desalination, Desalination, 216 (2007) 1–76.
[3] V.G. Molina, M. Busch and P. Sehn, Cost savings by novel seawater reverse osmosis elements and design concepts, Desal. Wat. Treat., 7 (2009) 160–177.
[4] Y.G. Lee, Y.S. Lee, J.J. Jeon, S. Lee, D.R. Yang, I.S. Kim and J.H. Kim, Artificial neural network model for optimizing operation of a seawater reverse osmosis desalination plant, Desalination, 249 (2009) 180–189.
[5] S.J. Kim, Y.G. Lee, K.H. Cho, Y.M. Kim, S. Choi, I.S. Kim, D.R. Yang and J.H. Kim, Site-specific raw seawater quality impact study on SWRO process for optimizing operation of the pressurized step, Desalination, 238 (2009) 140–157.
[6] S.J. Kim, S. Oh, Y.G. Lee, M.G. Jeon, I.S. Kim and J.H. Kim, A control methodology for the feed water temperature to optimize SWRO desalination process using genetic programming, Desalination, 249 (2009) 190–199.
[7] S.J. Kim, Y.G. Lee, S. Oh, Y.S. Lee, Y.M. Kim, M.G. Jeon, S. Lee, I.S. Kim and J.H. Kim, Energy saving methodology for the SWRO desalination process: control of operating temperature and pressure, Desalination, 249 (2009) 260–270.
[8] A. Zhu, P.D. Christofides and Y. Cohen, Minimization of energy consumption for a two-pass membrane desalination: Effect of energy recovery, membrane rejection and retentate recycling, J. Membr. Sci., 339 (2009) 126–137.
[9] M. Soltanieh and W.N. Gill, Review of reverse osmosis membrane and transport models, Chem. Eng. Commun., 12 (1981) 279–363.
[10] M.E. Williams, A review of reverse osmosis theory, www.eetcorp.com/heepm/RO_TheoryE.pdf, 2003.
[11] K.L. Chen, L. Song, S.L. Ong and W.J. Ng, The development of membrane fouling in full-scale RO processes, J. Membr. Sci., 232 (2004) 63–72.
[12] W. Zhou, L. Song and T.K. Guan, A numerical study on concentration polarization and system performance of spiral wound RO membrane modules, J. Membr. Sci., 271 (2006) 38–46.
[13] S. Sourirajan and T. Matsuura, Reverse Osmosis/Ultrafiltration Principles, National Research Council of Canada, Ottawa, Canada, 1985.
[14] C.R. Bouchard, P.J. Carreau, T. Matsuura and S. Sourirajan, Modeling of ultrafiltration: predictions of concentration polarization effects, J. Membr. Sci., 97 (1994) 215–229.
[15] C.J. Seeton, Viscosity–temperature correlation for liquids. Tribology Lett., 22 (2006) 67–78.
[16] U.S. Dept. of the Interior, Office of Saline Water Research and Development, Progress Report No. 363, September 1968.